

# Effect of colloidal charge discretization in the primitive model

René Messina\*, Christian Holm, and Kurt Kremer

*Max-Planck-Institut für Polymerforschung, Ackermannweg 10, 55128, Mainz, Germany*

(November 13, 2018)

## Abstract

The effect of fixed discrete colloidal charges in the primitive model is investigated for spherical macroions. Instead of considering a central bare charge, as it is traditionally done, we distribute *discrete* charges randomly on the sphere. We use molecular dynamics simulations to study this effect on various properties such as overcharging, counterion distribution and diffusion. In the vicinity of the colloid surface the electrostatic potential may considerably differ from the one obtained with a central charge. In the strong Coulomb coupling, we showed that the colloidal charge discretization qualitatively influences the counterion distribution and leads to a strong colloidal charge-counterion pair association. However, we found that *charge inversion* still persists even if strong pair association is observed.

PACS. 82.70.Dd Disperse systems: Colloids

PACS. 61.20.Qg Structure of associated liquids: electrolytes, molten salts, etc.

PACS. 41.20.-q Applied classical electromagnetism

Typeset using REVTeX

---

\*email: messina@mpip-mainz.mpg.de

## I. INTRODUCTION

The electrostatic interactions in charged colloidal systems play a crucial role in determining the physical properties of such materials [1,2]. The behavior of these systems is extremely complex due to the *long range* Coulomb interactions. A first simplifying assumption is to treat the solvent as a dielectric medium solely characterized by its relative permittivity  $\epsilon_r$ . A second widely used approximation consists in modeling the *short range* ion-ion excluded volume interaction by hard spheres. These two approximations are the basis of the so-called primitive model of electrolyte solutions. The system under consideration is an asymmetrical polyelectrolyte made up of highly charged macroions and small counterions in solution. A further simplification can be achieved by partitioning the system into subvolumes (cells), each containing one macroion together with its neutralizing counterions plus, if present, additional salt. This approximation has been called accordingly the cell model [3,4]. The cells assume the symmetry of the macroion, here spherical, and are electrostatically decoupled. In this way one has reduced a complicated many-body problem to an effective one colloid problem. For spherical macroions the structural charge is normally modeled by a *central* charge, which, by Gauss theorem, is equivalent of considering a *uniform* surface charge density as far as the electric field *outside* the sphere is concerned.

Most analytical work as well as simulation approaches rely on the above assumptions. It is well known that in the strong Coulomb coupling regime ion-ion correlations become very important, and significant deviations from mean-field approaches are expected. One of the effects which the mean-field theory like Poisson-Boltzmann can not explain is the phenomenon of overcharge, also called charge inversion. It consists of binding excess counterions to a charged particle (macroion) so that its net charge changes sign. This has recently attracted significant attention [5–14]. It may give rise to a possible mechanism for strong long range attraction between like-sign charged colloids [12,13].

The purpose of this paper is to investigate if such a phenomenon (overcharge) depends on the way the structural charge is represented. The macroion is taken to be perfectly

spherical, i. e. we neglect any surface roughness [15]. We introduce discrete charges on the macroion sphere instead of a central charge, and compare the results to those obtained with a central charge. We concentrate on the following properties in the strong Coulomb coupling: overcharging, counterion distribution and surface diffusion.

## II. SIMULATION MODEL

### A. Macroion charge discretization

The macroion charge discretization is produced by using  $N_m$  identical microions of diameter  $\sigma$ , all identical to the counterions, distributed *randomly* on the surface of the macroion. Then the structural charge is  $Q = -Z_m e = -Z_c N_m e$ , where  $Z_m > 0$ ,  $Z_c$  is the counterion valency and  $e$  is the positive elementary charge. The discrete colloidal charges (DCC) are *fixed* on the surface of the spherical macroion. In spherical coordinates the elementary surface is given by:

$$dA = r_0^2 \sin\theta d\theta d\varphi = -r_0^2 d(\cos\theta) d\varphi, \quad (1)$$

and to produce a random discrete charge distribution on the surface we generated randomly the variables  $\cos\theta$  and  $\varphi$ . Only configurations leading to an overlap of microions are rejected. Figure 1 shows a schematic view of the setup. Note that in real physical systems like sulfonated latex spheres, no large heterogeneities are expected in the charge distribution, provided that the colloid surface is relatively regular, therefore our choice is justified. Nevertheless, the experimental situation is more complicated since other phenomena such as surface chemical reactions [16], hydration, roughness [15] and many more may be present. Here, we restrict ourselves to a simple model in order to understand the effect of macroion charge discretization, and leave the other questions for future investigations.

## B. Molecular dynamics procedure

We use molecular dynamics (MD) simulations to compute the motion of the counterions coupled to a heat bath acting through a weak stochastic force  $\mathbf{W}(t)$ . The equation of motion of counterion  $i$  reads

$$m \frac{d^2 \mathbf{r}_i}{dt^2} = -\nabla_i U - m\Gamma \frac{d\mathbf{r}_i}{dt} + \mathbf{W}_i(t), \quad (2)$$

where  $m$  is the counterion mass,  $U$  is the potential force having two contributions: the Coulomb interaction and the excluded volume interaction and  $\Gamma$  is the friction coefficient. Friction and stochastic force are linked by the dissipation-fluctuation theorem  $\langle \mathbf{W}_i(t) \cdot \mathbf{W}_j(t') \rangle = 6m\Gamma k_B T \delta_{ij} \delta(t - t')$ . For the ground state simulations the fluctuation force is set to zero.

Excluded volume interactions are taken into account with a pure repulsive Lennard-Jones potential given by

$$U_{LJ}(r) = \begin{cases} 4\epsilon \left[ \left( \frac{\sigma}{r-r_0} \right)^{12} - \left( \frac{\sigma}{r-r_0} \right)^6 \right] + \epsilon, & \text{for } r - r_0 < r_{cut}, \\ 0, & \text{for } r - r_0 \geq r_{cut}, \end{cases} \quad (3)$$

where  $r_0 = 0$  for the microion-microion interaction (the microion can be a counterion or a DCC),  $r_0 = 7\sigma$  for the macroion-counterion interaction, and  $r_{cut} (= 2^{1/6}\sigma)$  is the cutoff radius. This leads to a macroion-counterion distance of closest approach  $a = 8\sigma$ . Energy and length units in our simulations are defined as  $\epsilon = k_B T_0$  (with  $T_0 = 298$  K), and  $\sigma = 3.57$  Å respectively.

The pair electrostatic interaction between any pair  $ij$ , where  $i$  and  $j$  denote either a DCC or a counterion, reads

$$U_{coul}(r) = k_B T_0 l_B \frac{Z_i Z_j}{r}, \quad (4)$$

where  $l_B = e^2 / 4\pi\epsilon_0 \epsilon_r k_B T_0$  is the Bjerrum length describing the electrostatic strength. Being essentially interested in the strong Coulomb coupling regime we choose the relative permittivity  $\epsilon_r = 16$  ( $l_B = 10\sigma$ ), *divalent* counterions ( $Z_c = 2$ ) and *divalent* DCC for the remaining of this paper.

The macroion and the counterions are confined in a spherical impenetrable cell of radius  $R$ . The macroion is held fixed and is located at the center of the cell. The colloid volume fraction  $f_m$  is defined as  $r_m^3/R^3$ , where  $r_m = a - \sigma/2$  is the colloid radius. We have fixed  $R = 40\sigma$  so that  $f_m = 6.6 \times 10^{-3}$ . To avoid image charge complications, the permittivity  $\epsilon_r$  is supposed to be identical within the whole cell (including the macroion) as well as outside the cell.

### III. MACROION ELECTRIC FIELD

The first step to understand the effect of colloidal charge discretization consists of estimating the electric field, or equivalently, the electrostatic *potential* generated by such a sphere in the *absence* of counterions. A simple graphical visualization of the field lines is here not possible, since there is no perfect symmetry. Indeed, in the present case the electric field becomes very anisotropic and irregular close to the sphere, which is the most interesting region where correlations are expected to be large. To describe qualitatively the effect of charge discretization on the electrostatic potential, we compute for three perpendicular directions  $x, y, z$  the resulting *radial* potentials  $V_x(r), V_y(r), V_z(r)$  (see Fig. 1) for one given DCC random distribution as a function of the distance  $r \geq a$  from the macroion center. The radial component of the electric field  $E_i(r) = -\frac{\partial}{\partial r}V_i(r)$  has the important feature of representing the *attractive* component towards the sphere. The normalized radial potential  $V_i$  in the  $i^{\text{th}}$  direction at a distance  $r$  from the colloid center is given by:

$$V_i(r) = -k_B T_0 l_B Z_c^2 \sum_{j=1}^{N_m} \frac{1}{|\mathbf{r}_j(r)|}, \quad (5)$$

where  $\mathbf{r}_j(r)$  is the vector pointing from the microion  $j$  to the point where the electric potential is computed (see Fig. 1). Physically,  $V(r)$  is the electrostatic potential interaction between a counterion and all the surface microscopic colloid charges. The monopole contribution is merely given by  $V_{mono}(r) = -k_B T_0 l_B \frac{Z_m Z_c}{r}$ . In Fig. 3 we show the electric potential for three typical bare charges, each corresponding to *one* given random macroion charge distribution.

For all cases, one notes that at the vicinity of the surface the potential becomes very different from the one computed with a central charge. We carefully checked that similar results were obtained for other choices of  $x$ ,  $y$ ,  $z$  directions (by rotating the trihedron  $(\mathbf{e}_x, \mathbf{e}_y, \mathbf{e}_z)$ ). However if we observe the electric field sufficiently far away from the colloidal surface (about one macroion diameter) the field is almost exactly the same as the one produced by a central charge, which we term *isotropic* for the rest of this paper. A closer look on Fig. 3 reveals that by increasing the bare charge  $Z_m$  the electric field starts to become isotropic at smaller distances from the sphere's surface. This last feature can be physically easily interpreted. In fact when one increases the bare charge, one also increases the absolute number of discrete charges which has the effect of approaching the uniform continuous charge density limit (corresponding to the isotropic case).

To capture the discretization effect on the *surface* electrostatic potential, we have measured the electrostatic potential along a circle of radius  $a$  concentric to the spherical macroion (see Fig. 1). We start from the top of a given DCC microion and move along a circle in a random direction and measure the electrostatic potential  $V(s)$  as a function of the arc length separation  $s$  from the starting point. The same formula as Eq. (5) has been used here. The *constant* monopole contribution is merely given by  $V_{mono} = -k_B T_0 l_B \frac{Z_m Z_c}{a}$ . Results are reported in Fig. 3 for the same configurations as before. It clearly shows that the electrostatic potential is strongly fluctuating. More specifically, the higher the structural charge  $Z_m$ , the larger the “oscillation frequency” of the potential fluctuations over the surface. This feature can be explained in terms of “holes”. In the very vicinity of a given DCC the potential is increased (in absolute value) in average, and around a given DCC there is a hole (depletion of charges) which tends to decrease the potential (in absolute value). The average surface of this hole is increasing with decreasing bare charge  $Z_m$  (i. e. decreasing density of charged sites).

In the following sections we are going to study the effect of charge discretization on the counterions distribution in the strong Coulomb coupling. For all following results we used the same random charge distributions which gave the results of Figs. 2 and 3.

## IV. GROUND STATE ANALYSIS

In this section, we focus on counterion distribution exclusively governed by *energy minimization*, i. e.  $T = 0\text{K}$ . In such a case correlations are maximal, and all the counterions lie on the surface of the spherical macroion. To avoid the trapping in metastable states, we systematically heat and cool (10 cycles) the system and retain the lowest energy state obtained in this way. Furthermore we choose as the starting configuration one where each DCC is exactly associated with one counterion, and each of these *dipoles* are radially oriented (each dipole vector and the macroion center lie on the same line). Preliminary, we checked that this method reproduces well the ground state energy and structure in simple situations where a central charge with two, three, four or five counterions is present. The structure of these systems is well known by the Gillespie rules [17]. It turns out that in these situations no rough energy landscape (even for  $Z_m = 180$  and 90 counterions) appears and therefore the MD simulation easily finds the global minimum. It is only in the case of DCC that several energy minima are observed.

### A. Neutral case

First we consider the simple salt free case where the system [macroion + counterions] is neutral. In order to characterize the counterion layer, we compute the counterion correlation function (denoted by CCF)  $g(r)$  on the surface of the sphere, defined as:

$$\rho_s^2 g(r) = \sum_{i \neq j} \delta(r - r_i) \delta(r - r_j), \quad (6)$$

where  $\rho_s = N_c/4\pi a^2$  is the surface counterion concentration ( $N_c = Z_m/Z_c$  being the number of counterions),  $r$  corresponds to the arc length on the sphere. Note that at zero temperature all equilibrium configurations are identical, thus only one is required to obtain the CCF. Similarly, one can also define a surface macroion correlation function (MCF) for the microions on the surface of the macroion. The CCF is normalized as follows

$$\rho_s \int_0^{\pi a} 2\pi r g(r) dr = (N_c - 1). \quad (7)$$

Because of the *finite* size and the topology of the sphere,  $g(r)$  has a cut-off at  $\pi a$  ( $=25.1 \sigma$ ). Therefore at “large” distance the correlation function differs from the one obtained with an infinite planar object.

The CCF and MCF for two different structural charges  $Z_m$  (50 and 180) can be inspected in Fig. 4. The CCF is computed for a system with a central charge (CC) and for the discrete colloid charges (DCC) case. One remarks that both CCF differ considerably following the nature of the colloidal charge, i. e., discrete or central (see Fig. 4). For the isotropic case (central charge) a Wigner Crystal structure is observed as was already found in Refs. [12,13,18]. It turns out that when we have to deal with DCC the counterion distribution is strongly dictated by colloidal charge distribution (see Fig. 4). Ground state structures are depicted in Fig. 5. It clearly shows the *ionic pairing*, between DCC and counterions. Also, it appears natural to call such a structure a *pinned* configuration. However one can expect that the structure might become less pinned if the typical intra-dipole distance (here  $\sigma$ ) and the typical mean inter-dipole distance become of the same order. This is a case which is not discussed in the present paper. It would correspond to extremely highly charged colloids that are rarely encountered in nature. Nevertheless, we checked that even for  $Z_m = 360$  the structure is still pinned, where the average inter-dipole distance is about  $2\sigma$ .

## B. Overcharge

We now investigate the overcharge phenomenon. The starting configurations corresponds to neutral ground states as were previously obtained. The spirit of this study is very similar to the one undertaken in Ref. [12]. To produce overcharge, one adds successively overcharging counterions (OC) at the vicinity of the colloidal surface. Thus the resulting system is no longer neutral. By using Wigner crystal theory [6,19], we showed that the gain in electrostatic energy (compared to the neutral state) by overcharging a single *uniformly* charged colloid can be written in the following way [12,13,18]:



$$\Delta E_n^{OC} = \Delta E^{cor} + \Delta E^{mon} = -n\gamma\sqrt{N_c} \left[ \frac{3}{2} + \frac{3n}{8N_c} \right] + (k_B T_0) l_B Z_c^2 \frac{(n-1)n}{2a}, \quad (8)$$

where  $\Delta E^{cor}$ , which is equal to the first term of the right member, denotes the gain in energy due to ionic correlations for  $n$  OC. The functional form of this term can be derived from WC theory [12,13,18]. The second term on the right hand side,  $\Delta E^{mon}$ , is the monopole repulsion, which sets in when the system is overcharged (with  $n > 1$ ). This term will, for sufficient high number  $n$  of OC, stops the process of overcharging. As before  $N_c = Z_m/Z_c$  is the number of counterions in the neutral state, and  $\gamma$  is a constant which was determined by using the measured value of  $\Delta E_1^{OC}$  of our simulations.

The total electrostatic energy of the system as a function of the number of OC is displayed Fig. 6 for four bare charges  $Z_m$  (50, 90, 180 and 360). These energy curves corresponding to discrete systems were produced by averaging over five random DCC realizations. Again, the overcharging process is affected by the charge discretization and pinning, but it is still energetically *favorable*. The main effects of charge discretization are: (i) the reduction of gain of energy and (ii) the reduction of maximal (critical) acceptance of OC. Both points can be explained in terms of *ion-dipole* interaction. It is exactly this *attractive* ion-dipole correlations which is responsible of charge inversion for colloidal systems with discrete charges. When the first OC is present, it is normally located in between the pinning centers, and will essentially interact with its neighboring dipoles (DCC-counterion). This interaction increases with decreasing OC-dipole separation, i. e. increasing colloid bare charge  $Z_m$ . This explains why the energy gained increases with  $Z_m$  (see Fig. 6). On the other, the repulsion between the counterions is not fully minimized since they do not adopt the ideal Wigner crystal structure that is obtained with a central charge which in turn explains (i). For a higher degree of overcharge, one has to take into account a repulsive monopolar contribution identical to  $\Delta E^{mon}$  appearing in Eq. (8). Again, since for DCC structures counterions are not perfectly ordered, the attractive correlational energy is smaller (in absolute value) than the one obtained with a central charge, which in turn explains (ii). Note that for very high bare charge ( $Z_m = 360$ ) the overcharge curve obtained with DCC approaches the one from

the continuous case as expected.

Common features of overcharging between isotropic and discrete systems are briefly given here. We note that the maximal (critical) acceptance of OC (4, 6 and 8 for a central charge and 2,4 and 6 for DCC) increases with the macroionic charge  $Z_m$  (50, 90 and 180 respectively). Furthermore, for a given number of OC, the gain in energy is always increasing with  $Z_m$ . Also, for a given macroionic charge, the gain in energy between two successive overcharged states is decreasing with the number of OC. Note that at  $T = 0$ , the value  $\epsilon_r$  acts only as a prefactor. All these features are captured by Eq. (8).

## V. FINITE TEMPERATURE

In this part, the system is brought to room temperature  $T_0$ . We are interested in determining the counterions distribution as well as the counterion motion within the counterion layer. The radius  $R$  of cell is again fixed to  $40\sigma$  so that the macroion volume fraction  $f_m$  has the *finite* value  $6.6 \times 10^{-3}$ . Under these conditions the system is still highly energy dominated so that at equilibrium all counterions lie on the surface of the macroion (strong condensation).

### A. Counterions distribution

Like in the ground state analysis, we characterize the counterion distribution via its surface correlation function. At non zero temperature, correlation functions are computed by averaging  $\sum_{i \neq j} \delta(r - r_i) \delta(r - r_j)$  over 1000 independent equilibrium configurations which are statistically uncorrelated. Results are depicted in Fig. 7. For both bare charges  $Z_m$  (50 and 180) considered the counterions distribution are affected by charge discretization. The effect of temperature is to smooth the CCF. As expected, for the central charge case, the counterion positional order is much weaker at room temperature than in the ground state case.

## B. Surface diffusion

The aim of this section is to answer the following question: do the counterions only oscillate around their equilibrium (ground state) position or do they have also a global translational motion over the sphere?

To answer to this question one introduces the following quantity:

$$\Delta x^2(t, t_0) = \frac{1}{t - t_0} \int_{t_0}^t dt' [x(t') - x(t_0)]^2, \quad (9)$$

which is referred as the *mean square displacement* (MSD), where  $x(t_0)$  represents the position of a given counterion at time  $t = t_0$  and  $x(t, t_0)$  is its position at later time  $t$ . The root mean square displacement (RMSD) is defined as  $\Delta x(t, t_0) = \sqrt{\Delta x^2(t, t_0)}$ . Like for the surface correlation function, the MSD is measured on the spherical surface (arc length) and it has a natural upper limit  $(\pi a)^2$ . Results for the discrete case are depicted in Fig. 8 for two macroion bare charges  $Z_m$  (50 and 180), where each counterion' RMSD is given. In both cases, the RMSD is smaller than the typical mean inter-dipole separation, which is approximatively  $(\rho_s)^{-1/2} \approx 6\sigma$  for  $Z_m = 50$  and  $(\rho_s)^{-1/2} \approx 3\sigma$  for  $Z_m = 180$ . This suggests that the motion of the counterion is *purely oscillatory* around its DCC pinning center. Fig. 8 also shows that pinning is stronger for  $Z_m = 50$  than for  $Z_m = 180$ . This is in agreement with our previous statement, where we point out that the inter-dipole distance has to be comparable (or smaller) to (than) the intra-dipole distance in order to reduce pinning effect. Thus the DCC sites do produce a noticeable energy well. One can get convinced on this point, by evaluating the electrostatic binding energy of an ionic pair  $E_{pin}$  which is

$$E_{pin} = -k_B T_0 l_B Z_c^2 / \sigma = -40 k_B T_0. \quad (10)$$

However, for much higher temperatures a liquid like behavior is to be expected. Also, of course, the strength of the pinning can be lowered by different parameters: larger ions, higher dielectric constant  $\epsilon_r$ , monovalent ions as it is captured by Eq. (10). For the isotropic case, we have checked that counterions have a large lateral motion and can move all over the sphere. This is obvious since in this situation there are no pinning centers.

## VI. CONCLUDING REMARKS

We have carried out MD simulations within the framework of the primitive model to elucidate the effect of colloidal charge discretization . The main result of our study is that, in the strong Coulomb coupling, the charge inversion is still effective when the macroion structural charge is carried by discrete charges distributed randomly over its surface area. We have shown that the intrinsic electrostatic potential solely due to the surface colloidal microions strongly vary from point to point on the macroion sphere. When counterions are present, it leads to a pinned structure where every counterion is associated with one colloidal charge site. Furthermore we observed a pure phonon-like behavior (counterion vibration with small lateral motion) is found at room temperature.

Future work will address the problem of valency asymmetry, that is when the colloidal charges are represented by monovalent counterions and the counterions are divalent. This is a non trivial situation since ionic pairing may be frustrated. Also, the case of the low Coulomb coupling regime should be addressed.

## ACKNOWLEDGMENTS

We thank B. Shklovskii for helpful and constructive remarks. This work is supported by *Laboratoires Européens Associés* (LEA).

## REFERENCES

- [1] J. Israelachvili, *Intermolecular and Surface Forces* (Academic, London, 1992).
- [2] D. F. Evans and H. Wennerström, *The Colloidal Domain* (Wiley-VCH, New York, 1999).
- [3] T. L. Hill, *Statistical mechanics* (Addison-Wesley, Reading, Mass., 1960).
- [4] H. Wennerström, B. Jönsson, and P. Linse, *J. Chem. Phys.* **76**, 4665 (1982).
- [5] V. Perel and B. Shklovskii, *Physica* **274A**, 446 (1999).
- [6] B. Shklovskii, *Phys. Rev. E* **60**, 5802 (1999).
- [7] E. M. Mateescu, C. Jeppesen, and P. Pincus, *Europhys. Lett.* **46**, 493 (1999).
- [8] J. F. Joanny, *Europ. J. Phys. B* **9**, 117 (1999).
- [9] E. Gurovitch and P. Sens, *Phys. Rev. Lett.* **82**, 339 (1999).
- [10] M. Lozada-Cassou, E. González-Tovar, and W. Olivares, *Phys. Rev. E* **60**, R17 (1999).
- [11] M. Deserno, C. Holm, and S. May, *Macromolecules* **33**, 199 (2000).
- [12] R. Messina, C. Holm, and K. Kremer, *Phys. Rev. Lett.* **85**, 872 (2000).
- [13] R. Messina, C. Holm, and K. Kremer, *Europhys. Lett.* **51**, 461 (2000).
- [14] T. T. Nguyen, A. Y. Grosberg, and B. I. Shklovskii, *J. Chem. Phys.* **113**, 1110 (2000).
- [15] S. Bhattacharjee, C. H. Ko, and M. Elimelech, *Langmuir* **14**, 3365 (1998).
- [16] O. Spalla and L. Belloni, *J. Chem. Phys.* **95**, 7689 (1991).
- [17] A theory that predicts molecular geometries using the notion that valence electron pairs occupy sites around a central atom in such a way as to minimize electron-pair repulsion. See for example D. W. Oxtoby, H. P. Gillis and N. H. Nachtrieb, *Principles of Modern Chemistry* (Saunders College Publishing, 1999), Chap. 3, p. 80.

[18] R. Messina, C. Holm, and K. Kremer, submitted.

[19] L. Bonsall and A. A. Maradudin, Phys. Rev. B **15**, 1959 (1977).

## FIGURES

FIG. 1. Schematic view of the setup: the discrete colloidal charges (DCC) of diameter  $\sigma$  are in dark grey. The radial electrostatic field components  $E_x$  and  $E_y$  are represented. For a detailed meaning of the other symbols see text. Note that this is a two-dimensional representation of the three-dimensional system.

FIG. 2. Radial electrostatic potential as a function of macroion center distance  $r$  produced by the fixed microscopic colloidal charges disposed on the sphere. These potentials have been measured in three perpendicular directions ( $x$ ,  $y$ ,  $z$ ) directions (see Fig. 1). The isotropic case corresponds to the field obtained with a central charge (monopole). Three structural charges are considered: (a)  $Z_m = 50$  (b)  $Z_m = 90$  and (c)  $Z_m = 180$ .

FIG. 3. Surface electrostatic potential as a function of the arc length  $s$  along a circle of radius  $a$  concentric to the macroion for three different trajectories. The monopole contribution is represented by the dashed line. The same configurations as those of Fig. 2(a-c) have been used.

FIG. 4. Ground state surface correlation functions for two macroion bare charges (a)  $Z_m = 50$  and (b)  $Z_m = 180$ . The two counterion correlation functions (CCF) are obtained for discrete colloidal charges (DCC) and for the central charge (CC). To get the same distance range for CCF and the colloidal surface discrete microions correlation function (MCF), the MCF curve x-axis ( $r/\sigma$ ) was rescaled by a factor  $a/r_0$  (compare setup Fig. 1).

FIG. 5. Ground state structures for two values (a)  $Z_m = 50$  and (b)  $Z_m = 180$  corresponding to the two cases of Fig. 4. The colloidal surface microions are in white, and the counterions in blue. Full ionic pairing association occurs.

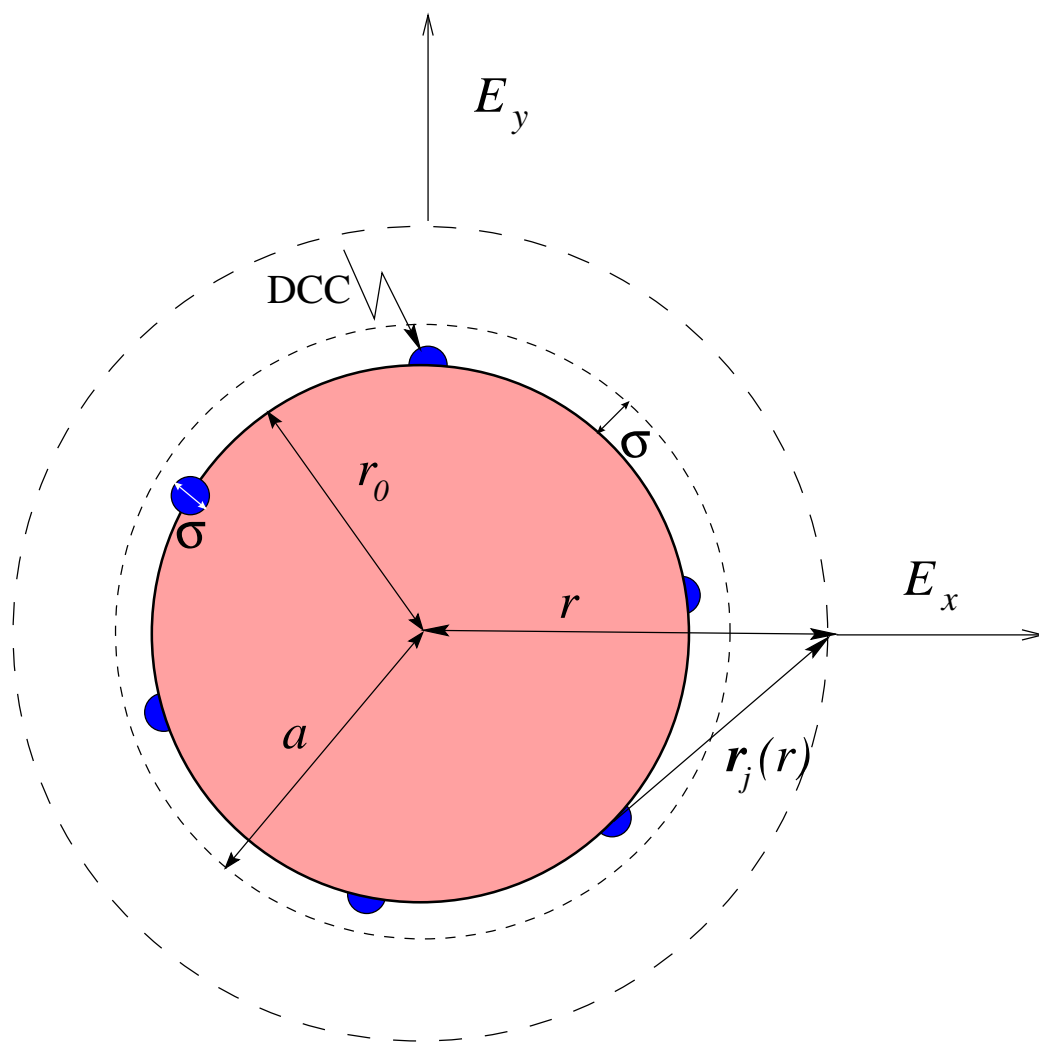
FIG. 6. Electrostatic energy (in units of  $k_B T_0$ ) for ground state configurations of a single charged macroion as a function of the number of *overcharging* counterions for three different bare charges  $Z_m$ . CC stands for the central charge case. The neutral case was chosen as the potential energy origin. Dashed lines are produced by using equation (8).

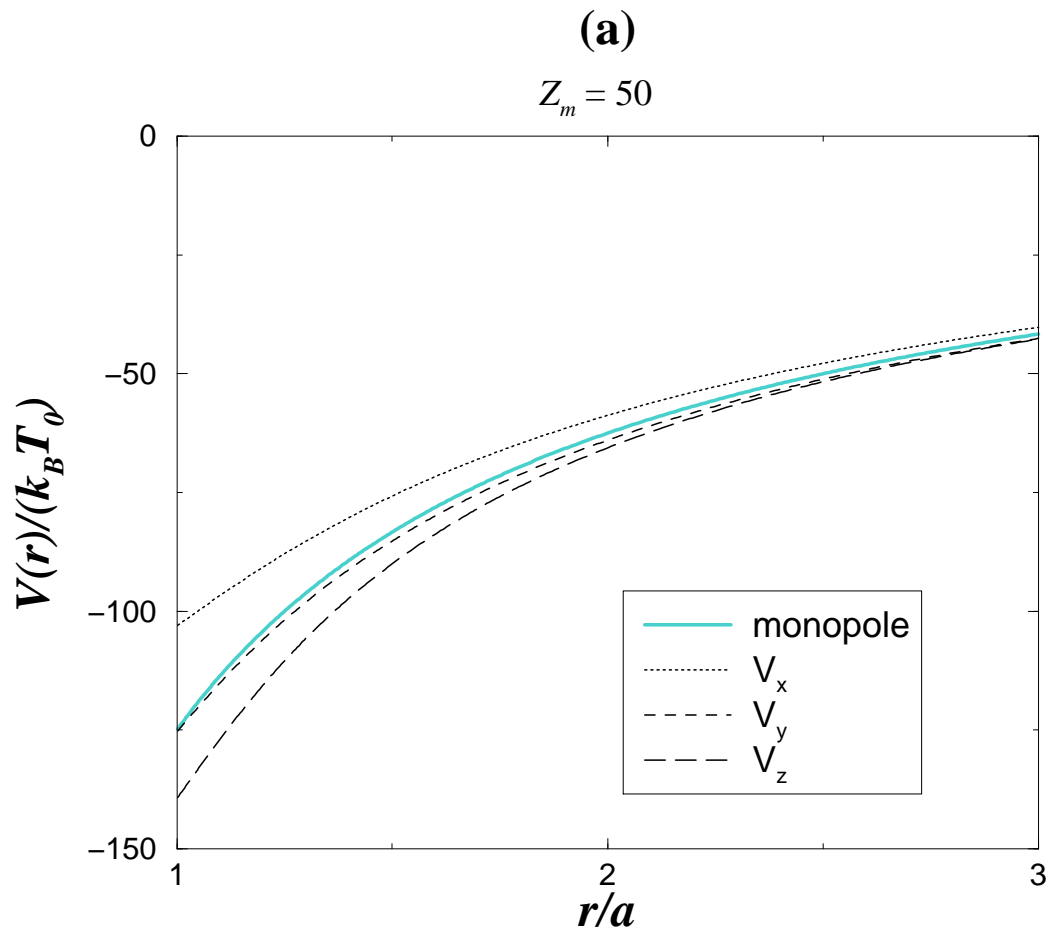
FIG. 7. Surface correlation functions at *room temperature*. The two CCF are obtained for discrete colloidal charges (DCC) and for the central charge (CC). (a)  $Z_m = 50$  (b)  $Z_m = 180$ .

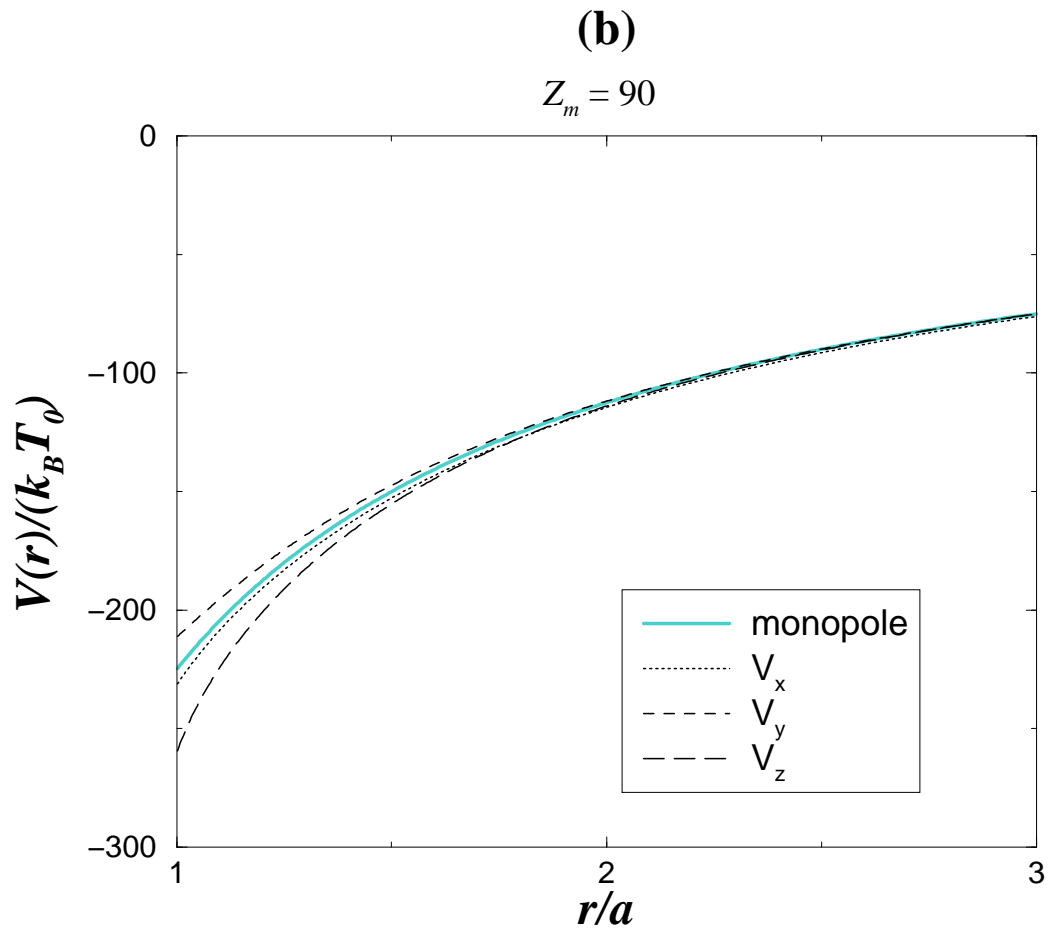
FIG. 8. Root mean square displacement (rmsd) for each counterion. (a)  $Z_m = 50$  (b)  $Z_m = 180$ .

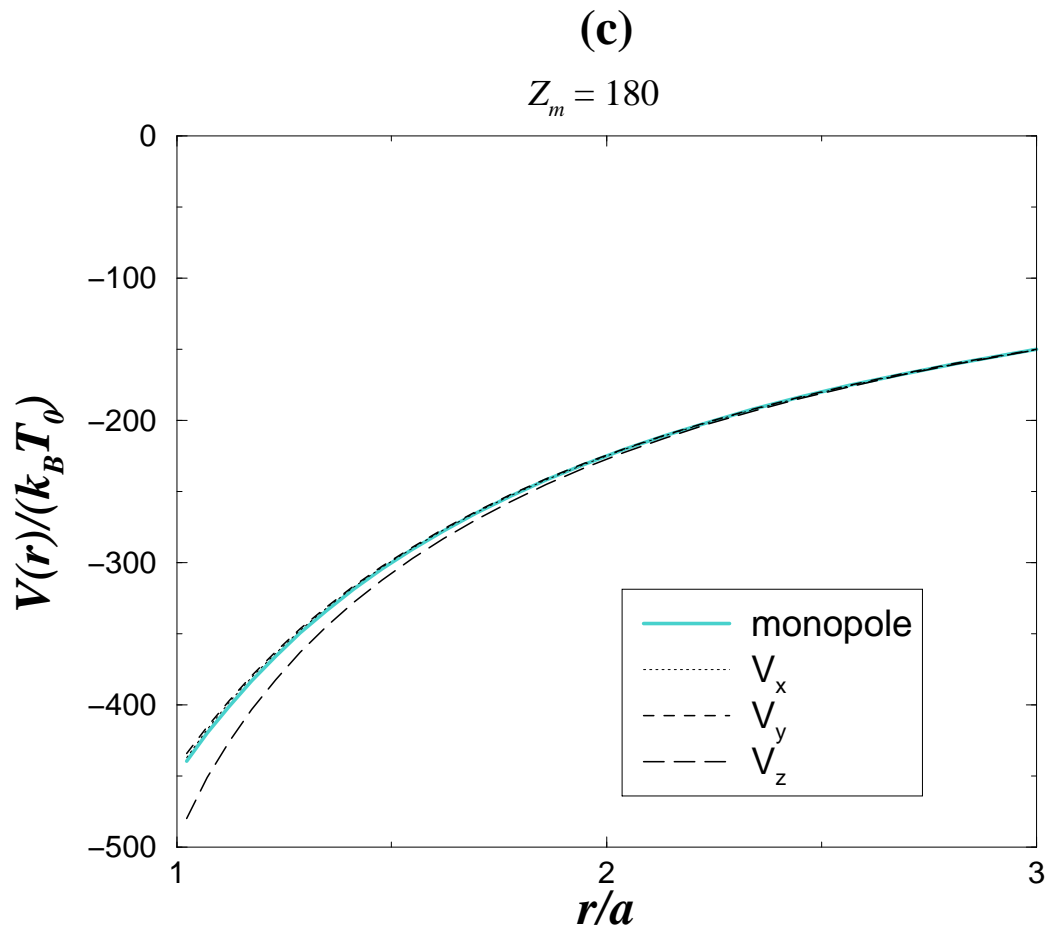


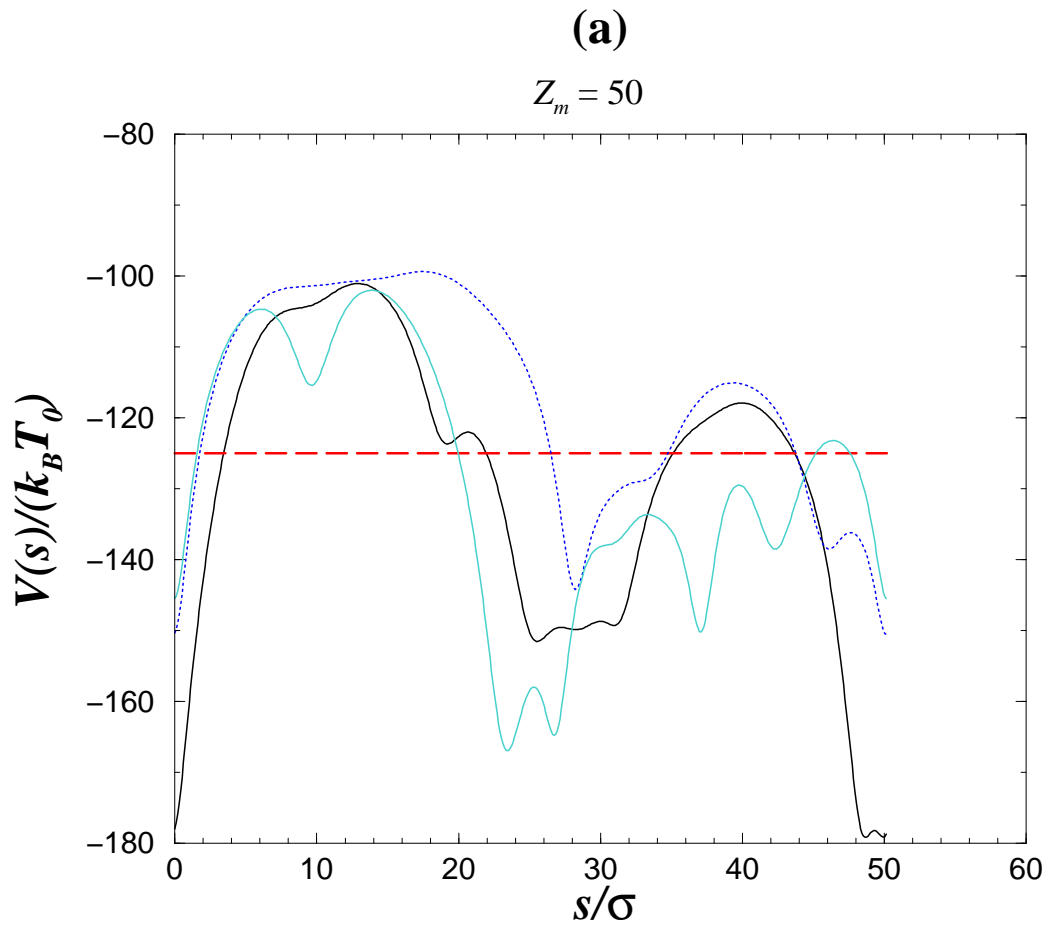
Messina et al.  
*European Physical Journal E*  
**Figure 1**

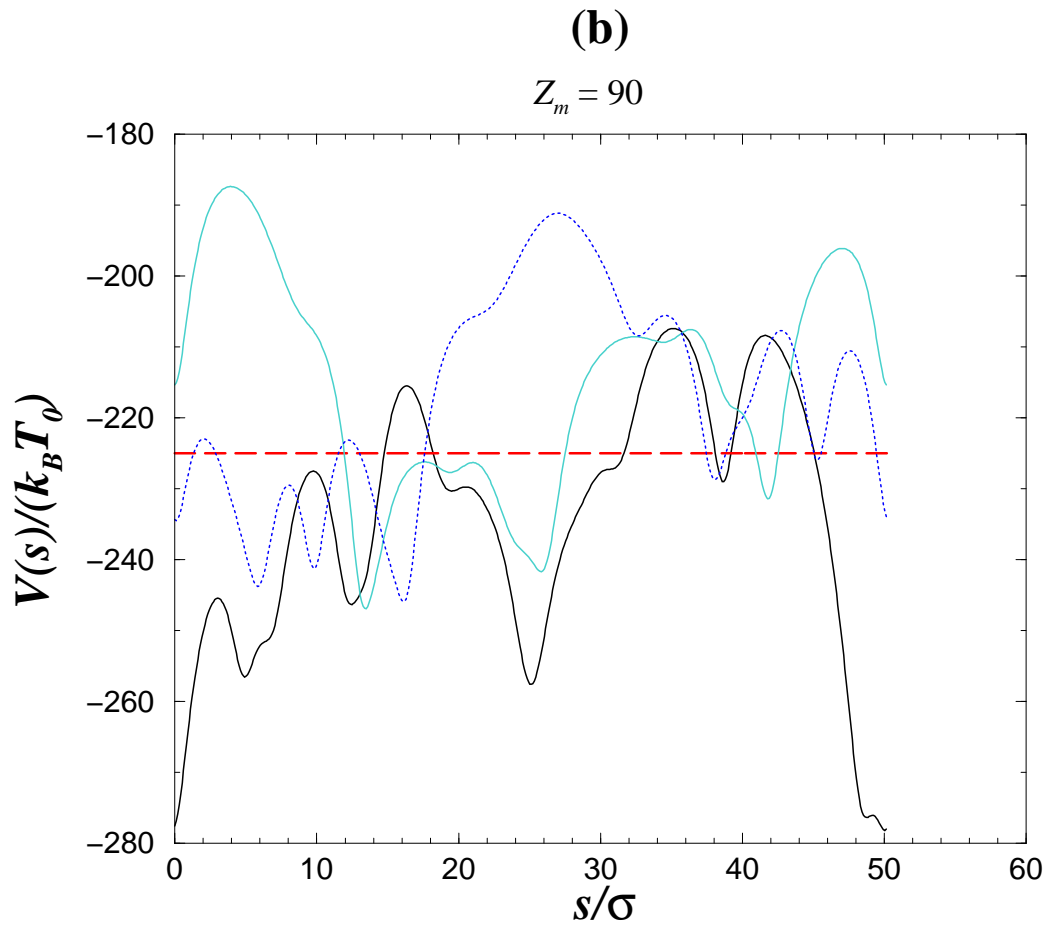




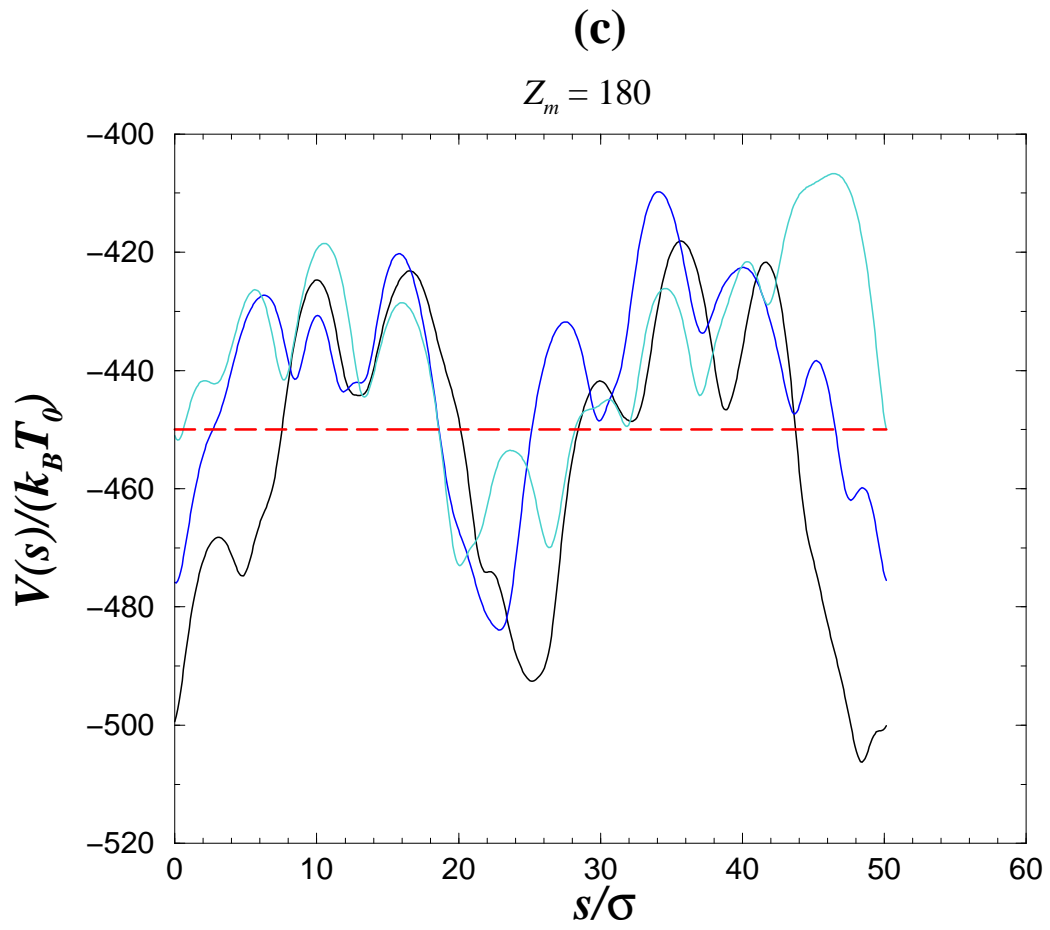


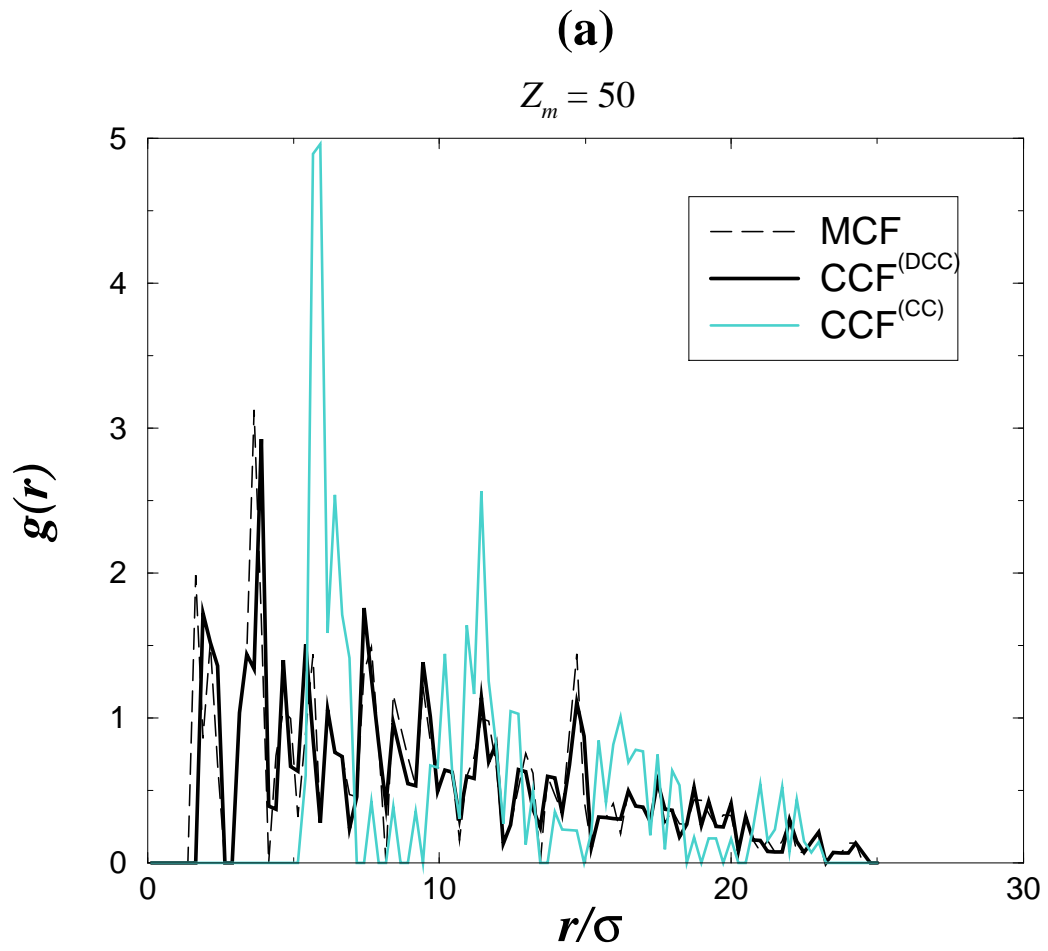




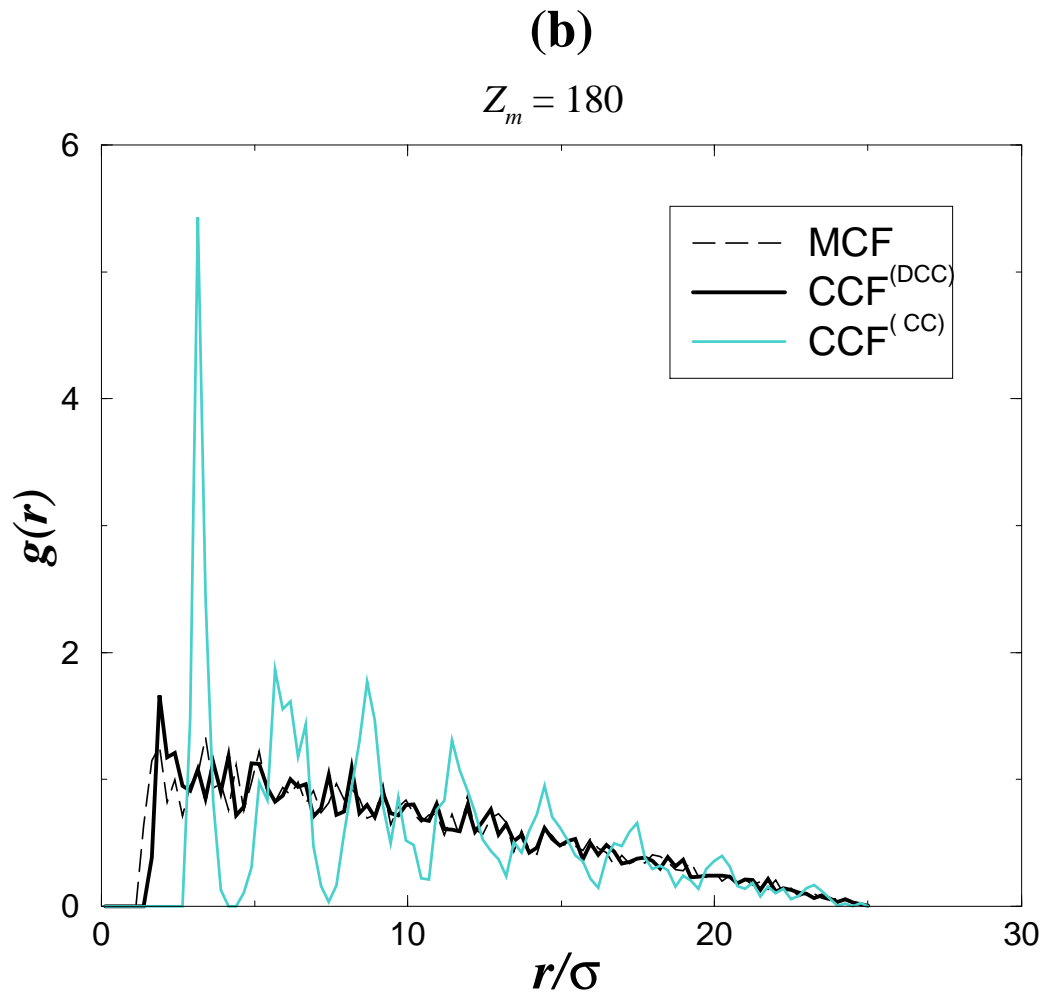


Messina et al.  
*European Physical Journal E*  
Figure 3 (c)

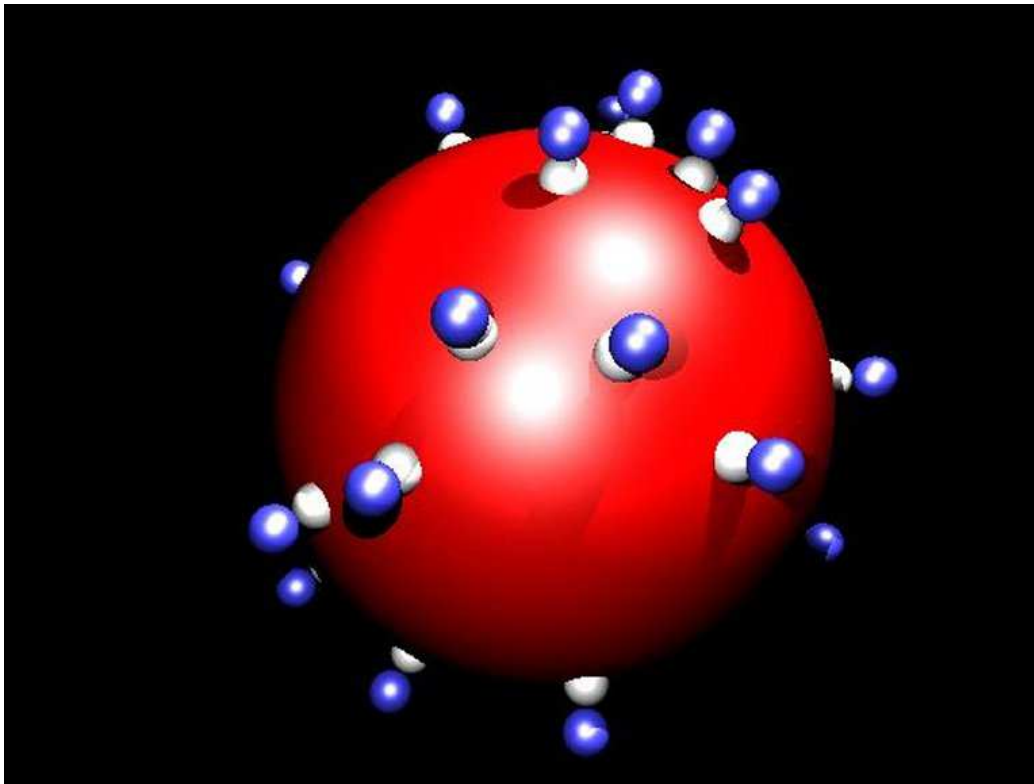




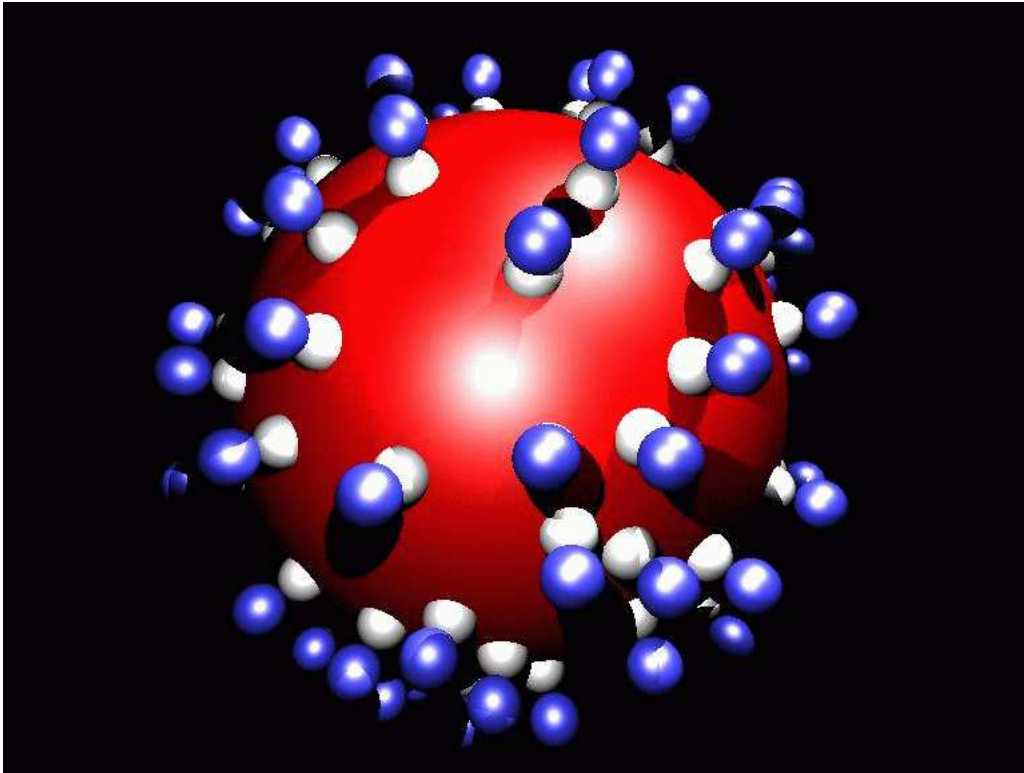




**Messina et al.**  
*European Physical Journal E*  
**Figure 5 (a)**  
(colored)



**Messina et al.**  
*European Physical Journal E*  
**Figure 5 (b)**  
(colored)



Messina et al.  
*European Physical Journal E*  
**Figure 6**

